Voltage-controlled switching and thermal effects in VO_2 nano-gap junctions

Arash Joushaghani,[1] Junho Jeong,[1] Suzanne Paradis,[2] David Alain,[2] J. Stewart Aitchison,[1] and Joyce K. S. Poon[1]

[1)]*Department of Electrical and Computer Engineering, University of Toronto, 10 King's College Road, Toronto, Ontario, M5S 3G4, Canada*

[2)]*Defence Research and Development Canada - Valcartier, 2459 Pie-XI Blvd. North, Quebec, Quebec G3J 1X5, Canada*

(Dated: 9 June 2014)

Voltage-controlled switching in lateral VO_2 nano-gap junctions with different gap lengths and thermal properties was investigated. The effect of Joule heating on the phase transition was found to be strongly influenced by the device geometry, the contact material, and the current. Our results indicate that the VO_2 phase transition was likely initiated electronically, which was sometimes followed by a secondary thermally-induced transition.

The metal-insulator phase transition in the correlated electron material[1], vanadium dioxide (VO_2), has attracted significant attention in optics[2–9] and electronics[10–15] for its applications in low power, compact and high speed switching. This is because the conductivity of the VO_2 can change by up to 5 orders of magnitude in response to external stimuli such as heating beyond 340 K[16], applied electric fields[17,18], surface charge accumulations[11], mechanical strain[19], and terahertz[20] or optical pulses[21]. Additionally, a main advantage of VO_2 is that a phase transition based on electronic reconfiguration can occur at picosecond time scales[21–23].

Many recent experiments have investigated the electronic phase transition in lateral[24–27] and vertical[28,29] VO_2 junctions. However, most time domain studies have shown switching times that are at best tens of nanoseconds[28,30,31], which suggest that the phase transition may be limited by thermal transients[32]. Although the possibility of a thermally induced phase transition is ruled out by heat transfer simulations of single crystalline[31–33] and polycrystalline VO_2 junctions[34], experiments indirectly measuring the local temperature of two terminal VO_2 junctions suggest that the temperature rose above the insulator-metal phase transition temperature of VO_2 at $T_{I\rightarrow M} = 340$ K[35,36]. These observations suggest that the role of thermal effects on the phase transition can vary significantly based on the parameters of the experiment. As a result, understanding these parameters not only sheds light on the nature of the phase transition, but may also help improve the electronically-induced switching times by showing how thermal effects may be suppressed.

In this work, we study the voltage-controlled switching of VO_2 lateral junctions with different lengths and contact metals to determine the electric field at the onset of phase transition at various heat dissipation rates. We show that when the current is low, the electric field at the onset of the insulator-metal transition is independent of the thermal conductivity and work function of the contact metal, but the reverse metal-insulator transition and hysteresis width are strongly dependent on the contact metal. Our results suggest that the phase transition is initiated electronically, which is sometimes accompanied by secondary thermal effects. The thermal contribution is determined by the device geometry, the contact metals, and the external load resistance. The variations of these parameters in different reports[26,32,35,36] help explain the discrepancy in the observed cause of the phase transition. Our results indicate that thermal effects may be reduced or potentially suppressed through device design.

We fabricated a series of lateral VO_2 junctions as illustrated in Fig. 1(a). A $t = 100$ nm VO_2 film was deposited using magnetron sputtering of a vanadium target on a 2 μm thick thermally grown SiO_2 on a Si substrate[3]. VO_2 lateral junctions were formed by electron beam lithography

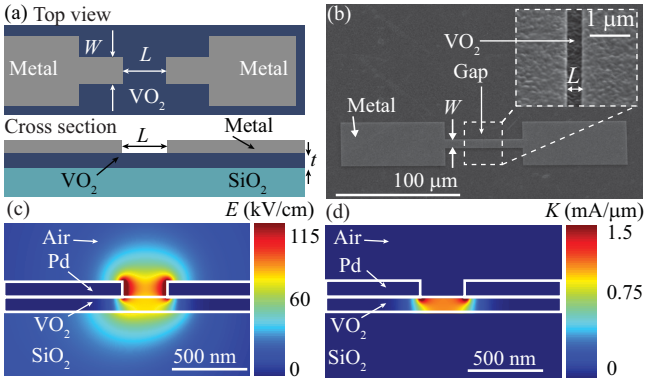

FIG. 1. (a) The top and side view schematic diagram of a VO_2 lateral junction. (b) A SEM of the device and the magnified image of the gap. (c) The simulated electric field profile and (d) current density profile when 3 V was applied over a 300 nm gap.

and lift-off of two metal contacts with a width of $W = 10$ μm, thickness of 100 nm, and a separation gap of length L. Figure 1(b) shows a scanning electron micrograph (SEM) of a device with a gap of 300 nm and palladium (Pd) contacts. The inset shows a magnified image of the gap.

When a voltage is applied between the two electrodes, an electric field establishes across the gap and a small current leaks through the VO_2 film. Figure 1(c) shows the simulated electric field profile when 3 V is applied across a 300 nm gap. Although a large portion of the field resides above the film in the air gap, the average field inside the VO_2 is 75 kV/cm. The field strength is consistent with the reported field values required to induce an electronic phase transition in VO_2[28,30]. Figure 1(d) shows the corresponding current density profile of Fig. 1(c) inside the VO_2 slab, which is mainly concentrated between the two electrodes.

Figure 2(a) shows a simplified circuit model of the device and experiment. The VO_2 junction (shaded area) is modeled as a capacitance, C_{Gap}, in parallel with a resistance, R_{Gap}. A voltage, V_{App}, was applied across each device and an external resistor R_{L} that limited the current. The current, I, and the voltage drop across the gap, V_{Gap}, were monitored. At a sufficiently high applied voltage, the insulator-metal transition would occur in the VO_2, resulting in a drop in the resistivity and an increase in the current.

Figure 2(b) shows I vs. V_{Gap} as V_{App} was ramped up (green line) and down (purple line) for a device with Pd contacts, $L = 300$ nm and $R_{\text{L}} = 550$ Ω. The numbered arrows in the figure trace V_{Gap}. For small values of V_{App} at point (1), the VO_2 was in the high resistivity phase, so the current increased slowly with voltage. At point (2), the voltage increased beyond the insulator-metal phase transition voltage, $V_{I\rightarrow M}$, so the resistivity of the VO_2 reduced, resulting in a sharp increase in the

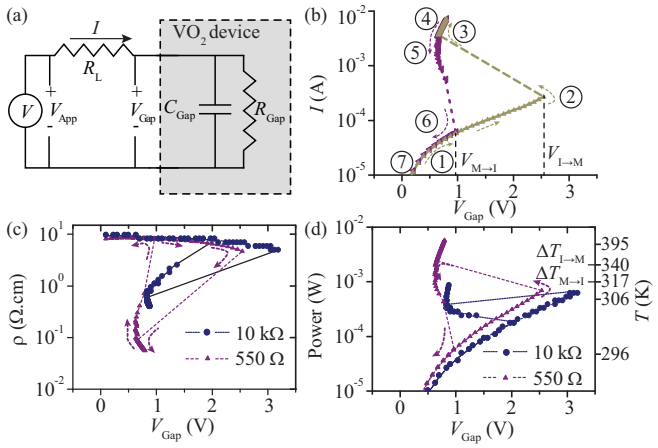

FIG. 2. (a) The simplified circuit model of the device and experiment. The (b) voltage-current,(c) voltage-resistivity, and (d) voltage-power relationship of a junction with a gap length of 300 nm and Pd contacts.

current accompanied by a drop in V_{Gap}, or a large negative differential resistance. After point (3), the VO_2 was in a low resistivity phase, and the current increased linearly with the applied voltage. When V_{App} was reduced back to zero between points (5) to (7), the curve traced a different path due to the hysteresis of VO_2. As V_{App} was reduced, V_{Gap} increased until point (6) when it reached the metal-insulator transition voltage, $V_{M\rightarrow I}$, after which the VO_2 returned to its high resistivity phase.

Figure 2(c) shows the resistivity of the underlying VO_2 film calculated as $\rho = R_{\text{Gap}}Wt/L$ when $R_{\text{L}} = 550\ \Omega$ and $10\ \text{k}\Omega$. For both values of R_{L}, ρ was relatively constant for small values of V_{Gap}, but it dropped significantly when V_{Gap} exceeded $V_{I\rightarrow M}$, and increased to its original value when V_{Gap} was reduced below $V_{M\rightarrow I}$. As expected, the initial value of ρ was independent of R_{L}, but $V_{I\rightarrow M}$ and the magnitude of the drop in ρ were dependent on R_{L}. As we shall show, this dependence stems from different Joule heating of the VO_2 slab[37].

To examine the Joule heating effects in our devices, we calculated the dissipated electrical power in the device by $P = I \times V_{\text{Gap}}$. Taking P to be the Joule heat source, we simulated the expected temperature in VO_2. Figure 2(d) shows P (left axis) and the simulated temperature[36], T, (right axis) of the VO_2 slab as a function of V_{Gap}. The simulated temperature is below $T_{I\rightarrow M} = 340$ K at the onset of the phase transition for both values of R_{L}, indicating that Joule heating alone would not be sufficient to initiate the phase transition. However, for $R_{\text{L}} = 550\ \Omega$ and at any given V_{Gap}, the simulated temperature in VO_2 is higher than that of $R_{\text{L}} = 10\ \text{k}\Omega$ which would lower $V_{I\rightarrow M}$. This temperature-induced decrease in $V_{I\rightarrow M}$ has been observed in bulk VO_2 films and has been studied by many groups for the electrical[27,34,36,38], optical[39] and strain induced phase

transitions[19]. For our devices, we found that when R_{L} was 10 kΩ, an increase in temperature of 8 K would result in the same $V_{I\rightarrow M}$ as the case when $R_{\mathrm{L}} = 550\ \Omega$. This value agrees well with the simulated temperature increase of 6.5 K, as shown in Fig. 2(d).

Joule heating can also explain the difference in the magnitudes of the resistivity drop after the phase transition for the two values of R_{L}. P at the onset of the transition was similar for both values of R_{L}, indicating that the same energy was required to initiate the phase transition. However, the change in P, and consequently T, after the transition was negative when $R_{\mathrm{L}} = 10$ kΩ and positive when $R_{\mathrm{L}} = 550\ \Omega$. For the case of $R_{\mathrm{L}} = 550\ \Omega$, the increase in P after the transition would lead to a rise in temperature of the VO_2 slab above $T_{I\rightarrow M} = 340$ K, which could initiate a secondary thermally-induced phase transition. The thermal transition has been shown to exhibit a larger resistivity switching magnitude than the electronic transitions[28]. Thus, a thermal transition would account for the larger change in ρ. This change in ρ was consistent with thermal resistivity switching of our bulk films. When $R_{\mathrm{L}} = 10$ kΩ, however, the decrease in P after the transition would lead to a decrease in the temperature, which would account for a smaller change in ρ.

The simulated temperatures before and after the phase transition for the two values of R_{L} suggest that the phase transition was most likely initiated electronically and was accompanied by secondary thermal effects. To verify that the phase transition was not initiated by Joule heating, we fabricated four sets of devices with different thermal dissipation rates using metals with different thermal conductivities as the contacts. This allowed us to vary the heat dissipation rate of the devices while keeping the heat generation rate constant. Since different contact metals would lead to different work functions mismatches and VO_2-metal interface resistances, we swept L to extrapolate the electric field at the onset of the transition and remove any work function differences at the metal-VO_2 interfaces.

DC measurements similar to those of Fig. 2 were conducted on samples with Pd, gold (Au), silver (Ag), or copper (Cu) contacts. All samples were made from the same VO_2 film. They all had a width of $W = 10\ \mu$m, a metal thickness of 100 nm and a separation gap of length L, which varied between 150 nm to 1000 nm. R_{L} was fixed at 10 kΩ. Figure 3(a) shows the measured $V_{I\rightarrow M}$ for various values of L (scattered points) and the corresponding linear fits (dashed lines) for each contact metal. The error bars represent the standard deviation in $V_{I\rightarrow M}$ for multiple measurements. The y-intercepts of Fig. 3(a) ($V_{I\rightarrow M}$ as $L \rightarrow 0$) are related to the work function difference at the metal-VO_2 interface due to the interface resistance and the work function difference between the

VO_2 and the contact metal. The intercepts of these plots are 2.2 $\pm$ 0.2 V for Pd , 2.3 $\pm$ 0.3 V for Au, 3.3 $\pm$ 0.5 V for Ag, and 3.2 $\pm$ 0.3 V for Cu. The order of these values correlates with the work function differences between the metal and that of VO_2 reported in Ref.[40]. After the phase transition, these interface effects decrease due to both the change in the VO_2 work function and the increase in carrier density. These measurements also show that neglecting interface effects results in an overestimation of the transition electric field by up to 63 % for a gap length of 300 nm. Although these interface effects may be negligible for $L \geq 1$ μm, they can lead to significant power dissipation in nanometer scale junctions. Doping may be used to create ohmic contacts to suppress these interface effects.

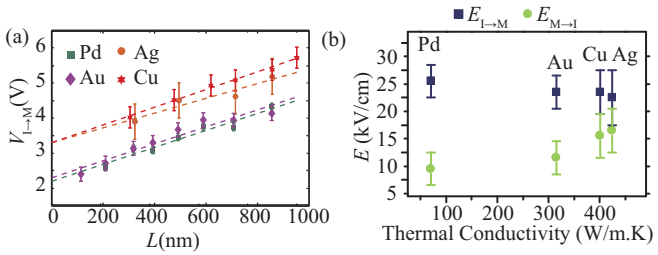

FIG. 3. (a) The forward transition voltage ($V_{I\to M}$) of devices with different thermal dissipation rates. (b) The electric field at the onset of phase transition for the forward and reverse transitions as the function of metal thermal conductivity.

As a measure of the "average" electric fields in the gap for the forward ($E_{I\to M}$) and reverse ($E_{M\to I}$) phase transitions, we calculate the slopes of $V_{I\to M}$ and $V_{M\to I}$ vs. L. Figure 3(b) shows $E_{I\to M}$ and $E_{M\to I}$ as a function of the thermal conductivity of the contact metal[41]. We found that the values of $E_{I\to M}$ were similar for the different contact metals despite their vastly different thermal conductivities, indicating that the forward transition was unlikely to be thermally-induced. If the transition was thermally initiated, the Pd devices with the lowest thermal conductivity would have required the smallest value of $E_{I\to M}$ for the phase transition, which was clearly not the case.

On the other hand, $E_{M\to I}$ was strongly dependent on the metal thermal conductivity, which can be explained by the dissipated power and temperature of the VO_2 after the phase transition as in Fig. 2(d). For $R_{\rm L} = 10$ kΩ, the dissipated power decreased at the onset of the phase transition. Well after the phase transition, however, the metallic VO_2 acted as a resistive heating element that raised the temperature with increasing voltage. At a sufficiently high power density, the local temperature of VO_2 could be higher than the metal-insulator phase transition temperature, $T_{M\to I}$ = 317 K. Consequently, the reverse phase transition was dominated by thermal dissipation rates, which occurred at lower $E_{M\to I}$ values for metals with lower thermal conductivities. Therefore,

devices that used contact metals with higher thermal conductivities exhibited smaller electric field hysteresis widths. It should be noted that the value of $E_{M\to I}$ is generally lower than $E_{I\to M}$, due to the hysteresis of VO_2 and the change in thermal conductivity of VO_2 after the phase transition. The temperature dependence of the electronic transition explains the observed dependence of $V_{I\to M}$ on the external load as shown in this work and similarly in Ref.[37]. For small values of $R_{\rm L}$, compared to the VO_2 channel resistance, the jump in the power density at the onset of the phase transition can substantially raise the temperature, resulting in strong thermal contributions to the phase transition.

TABLE I. Comparison of thermal effects in the voltage switching of recent two terminal VO_2 switches.

No.	**VO_2 Film Properties**					**Device Geometry**				**Properties at $I\to M$ Phase transition**		
	Deposition Technique	**Substrate**	**Film thickness (nm)**	**ρ (Ω.cm) (insulating phase)**	**ρ ratio $\frac{\text{Max}(\rho)}{\text{Min}(\rho)}$**	**L (μm)**	**W (μm)**	**R_L (kΩ)**	**Contact**	**$(E_{I\to M})^a$ (kV/cm)**	**Power density (μW/μm^3)**	**Temperature increase (K)**
1[b]	Sputtering	SiO_2	100	2	100	0.5	10	10	Pd	21[c]	0.42	17
									Au	23[c]	0.46	12
									Cu	23[c]	0.46	11
								0.5	Pd	20[c]	0.6	18
2[d]	Sputtering	Al	370	-	146	0.37	300	-	Ti/Au	50	5.5×10^{-5}	-
3[e]	Sputtering	SiO_2	200	0.2	80	16	8	0.2	Au	5	1.875	77[f]
4[g]	Sputtering	Al_2O_3	130	4	1000	20	50	180	Au	20	0.2	17 [f]
5[h]	Sole Gel	Al_2O_3	100	0.2	200	10	10	15	Ni	10	0.5	27
6[i]	Pulsed Laser Deposition	Al_2O_3	100	-	-	25	30[j]	1	Pt	12	4	180
7[k]	Evaporation of V	Al_2O_3	90	0.002	400	0.15	10	0.05	Ti/Au	9	0.5	-

[a] The $V_{I\to M}/L$ value, unless otherwise specified. [b] This work. [c] Extrapolated from the slope of $V_{I\to M}$ vs. L.
[d] Reference[25]. [e] Reference[33]. [f] Experimentally measured value.
[g] Reference[32]. [h] Reference[30]. [i] Reference[34].
[j] Width of the observed filament. [k] Reference[27].

Table 1 summarizes the VO_2 film properties, the device geometry and the estimated contribution of electrical and thermal effects in this work and other recent experiments on electrical switching of VO_2. The properties of VO_2 are also provided for comparison, where $\rho_{\rm I}$ is the resistivity of the insulating phase and ρ ratio is $\text{Max}(\rho)/\text{Min}(\rho)$. The device geometry and external load resistance have strong effects on the temperature increase in these devices. The reported temperature increase is directly proportional to the power density and provides a metric for comparison. Devices with small cross-sections and low loads have high dissipated power densities and consequently large temperature increases. Similarly, in our work, when $R_{\rm L}$ was reduced, the temperature at the onset of the phase transition increased. Devices with higher temperatures at the

phase transition generally required a lower $E_{I\rightarrow M}$. This is expected as increasing the temperature increases the carrier density inside the VO_2 and consequently reduces $E_{M\rightarrow I}$[38]. It should be noted that devices (3) and (6) had small cross-section areas and long gaps, which created sufficiently high power densities to increase the VO_2 temperature beyond $T_{I\rightarrow M}$. In these cases, the observed phase transitions were mostly thermally-induced.

In our experiments, although the transition was initiated electrically, it remains unclear whether the phenomenon was a field[17], a current or an avalanche effect[34]. Our preliminary experiments on electric field switching in similar structures, where the current was completely suppressed using a thin high-k dielectric that separated the contacts and the VO_2, showed that a purely electric-field induced switching could not be achieved at similar field strengths. The high-k dielectric typically experienced catastrophic breakdown before the VO_2 phase transition occurred.

In conclusion, we have demonstrated that voltage controlled switching in two terminal VO_2 switches in the nano-scale is dominated by electronic effects if the current could be suppressed. A large current causes a rapid increase in the power density after the phase transition to result in a secondary thermal transition. High frequency circuits for current regulation after the phase transition may be a solution to suppress secondary thermal effects. These circuits are typically used for current quenching in avalanche photo-diodes[42] and can be adapted to VO_2 devices to achieve picosecond switching times[22,23].

REFERENCES

[1]D. N. Basov, R. D. Averitt, D. van der Marel, M. Dressel, and K. Haule, Rev. Mod. Phys. **83**, 471 (2011).

[2]M. A. Kats, D. Sharma, J. Lin, P. Genevet, R. Blanchard, Z. Yang, M. M. Qazilbash, D. N. Basov, S. Ramanathan, and F. Capasso, Appl. Phys. Lett. **101**, 221101 (2013).

[3]A. Joushaghani, B. A. Kruger, S. Paradis, D. Alain, J. Stewart Aitchison, and J. K. S. Poon, Appl. Phys. Lett. **102**, 061101 (2013).

[4]M. D. Goldflam, T. Driscoll, B. Chapler, O. Khatib, N. M. Jokerst, S. Palit, D. R. Smith, B.-J. Kim, G. Seo, H.-T. Kim, M. Di Ventra, and D. N. Basov, Appl. Phys. Lett. **99**, 044103 (2011).

[5]B. A. Kruger, A. Joushaghani, and J. K. S. Poon, Opt. Express **20**, 23598 (2012).

[6]J. D. Ryckman, V. Diez-Blanco, J. Nag, R. E. Marvel, B. K. Choi, R. F. Haglund, and S. M. Weiss, Opt. Express **20**, 13215 (2012).

[7]R. M. Briggs, I. M. Pryce, and H. A. Atwater, Opt. Express **18**, 11192 (2010).

[8]A. Hache, B. Abdel Samad, M. Chaker, A. Herndaoui, and S. Vigne, in *CLEO 2013*, OSA Technical Digest (online) (Optical Society of America, San Jose, California, 2013) p. JW2A.56.

[9]H. Jerominek, D. Vincent, and F. Picard, Opt. Eng. **32**, 2092 (1993).

[10]J. Jeong, N. Aetukuri, T. Graf, T. D. Schladt, M. G. Samant, and S. S. P. Parkin, Science **339**, 1402 (2013).

[11]M. Nakano, K. Shibuya, D. Okuyama, T. Hatano, S. Ono, M. Kawasaki, Y. Iwasa, and Y. Tokura, Nature **487**, 459 (2012).

[12]Y. Zhou and S. Ramanathan, Crit. Rev. Solid State Mater. Sci. **38**, 286 (2013).

[13]Z. Yang, C. Ko, and S. Ramanathan, Annual Review of Materials Research **41**, 337 (2011).

[14]T. Driscoll, H.-T. Kim, B.-G. Chae, M. Di Ventra, and D. N. Basov, Appl. Phys. Lett. **95**, 043503 (2009).

[15]K. Hyun-Tak, C. Byung-Gyu, Y. Doo-Hyeb, M. Sung-Lyul, K. Gyungock, K. Kwang-Yong, and L. Yong-Sik, New J. Phys. **6**, 52 (2004).

[16]C. N. Berglund, IEEE Trans. Elec. Dev. **16**, 432 (1969).

[17]G. Stefanovich, A. Pergament, and D. Stefanovich, J. Phys. Condens. Matter **12**, 8837 (2000).

[18]D. Ruzmetov, G. Gopalakrishnan, C. Ko, V. Narayanamurti, and S. Ramanathan, J. Appl. Phys. **107**, 114516 (2010).

[19]J. Cao, E. Ertekin, V. Srinivasan, W. Fan, S. Huang, H. Zheng, J. W. L. Yim, D. R. Khanal, D. F. Ogletree, J. C. Grossman, and J. Wu, Nat Nano **4**, 732 (2009).

[20]M. Liu, H. Y. Hwang, H. Tao, A. C. Strikwerda, K. Fan, G. R. Keiser, A. J. Sternbach, K. G. West, S. Kittiwatanakul, J. Lu, S. A. Wolf, F. G. Omenetto, X. Zhang, K. A. Nelson, and R. D. Averitt, Nature **487**, 345 (2012).

[21]A. Cavalleri, C. Toth, C. W. Siders, J. A. Squier, F. Raksi, P. Forget, and J. C. Kieffer, Phys. Rev. Lett. **87**, 237401 (2001).

[22]K. Appavoo, B. Wang, N. F. Brady, M. Seo, J. Nag, R. P. Prasankumar, D. J. Hilton, S. T. Pantelides, and R. F. Haglund, Nano Lett. **14**, 1127 (2014).

[23]S. Lysenko, V. Vikhnin, A. Ra, F. Fernndez, and H. Liu, Phys. Rev. B **82**, 205425 (2010).

[24]K. Changhyun and S. Ramanathan, Appl. Phys. Lett. **93**, 252101 (2008).

[25]J.-G. Ramrez, R. Schmidt, A. Sharoni, M. E. Gmez, I. K. Schuller, and E. J. Patio, Appl. Phys. Lett. **102**, 063110 (2013).

[26]K. M. Martens, I. P. Radu, G. Rampelberg, J. Verbruggen, S. Cosemans, S. Mertens, X. Shi,

M. Schaekers, C. Huyghebaert, S. De-Gendt, C. Detavernier, M. Heyns, and J. A. Kittl, ECS Trans. **45**, 151 (2012).

[27]B. Simon Mun, J. Yoon, S.-K. Mo, K. Chen, N. Tamura, C. Dejoie, M. Kunz, Z. Liu, C. Park, K. Moon, and H. Ju, Appl. Phys. Lett. **103**, (2013).

[28]Z. You, C. Xiaonan, K. Changhyun, Y. Zheng, C. Mouli, and S. Ramanathan, IEEE Elec. Dev. Lett. **34**, 220 (2013).

[29]S. Giwan, K. Bong-Jun, K. Changhyun, C. Yanjie, L. Yong Wook, S. Jun-Hwan, S. Ramanathan, and K. Hyun-Tak, IEEE Elec. Dev. Lett. **32**, 1582 (2011).

[30]J. Leroy, A. Crunteanu, A. Bessaudou, F. Cosset, C. Champeaux, and J.-C. Orlianges, Appl. Phys. Lett. **100**, 213507 (2012).

[31]S. D. Ha, Y. Zhou, C. J. Fisher, S. Ramanathan, and J. P. Treadway, J. Appl. Phys. **113**, (2013).

[32]Y. Zhang and S. Ramanathan, Solid-State Electron. **62**, 161 (2011).

[33]G. Gopalakrishnan, D. Ruzmetov, and S. Ramanathan, Journal of Materials Science **44**, 5345 (2009).

[34]T. Driscoll, J. Quinn, M. Di Ventra, D. N. Basov, G. Seo, Y.-W. Lee, H.-T. Kim, and D. R. Smith, Phys. Rev. B **86**, 094203 (2012).

[35]A. Zimmers, L. Aigouy, M. Mortier, A. Sharoni, S. Wang, K. G. West, J. G. Ramirez, and I. K. Schuller, Phys. Rev. Lett. **110**, 056601 (2013).

[36]S. Kumar, M. D. Pickett, J. P. Strachan, G. Gibson, Y. Nishi, and R. S. Williams, Advanced Materials **25**, 6128 (2013).

[37]S. B. Lee, K. Kim, J. S. Oh, B. Kahng, and J. S. Lee, Appl. Phys. Lett. **102**, 063501 (2013).

[38]A. L. Pergament, P. P. Boriskov, A. A. Velichko, and N. A. Kuldin, J. Phys. Chem. Solids **71**, 874 (2010).

[39]Z. Tao, T.-R. T. Han, S. D. Mahanti, P. M. Duxbury, F. Yuan, C.-Y. Ruan, K. Wang, and J. Wu, Phys. Rev. Lett. **109**, 166406 (2012).

[40]C. Ko, Z. Yang, and S. Ramanathan, ACS Applied Materials and Interfaces **3**, 3396 (2011).

[41]W. M. Haynes, *Handbook of Chemistry and Physics*, 94th ed. (CRC, 2013).

[42]S. Cova, M. Ghioni, A. Lacaita, C. Samori, and F. Zappa, Applied Optics **35**, 1956 (1996).